The Probability Distribution of the Fab–Fab Angles: A Coherence Test of the Model

In this appendix we study the distribution of the Fab–Fab angles, which we label with $\rho_3(\xi)$. The experimental profile is shown in Fig. 1 *a* inset: It displays a clear bell–shaped trend with a peak in the region $[100^\circ, 120^\circ]$. Correspondingly, the cumulative distribution follows a characteristic sigmoid trend.

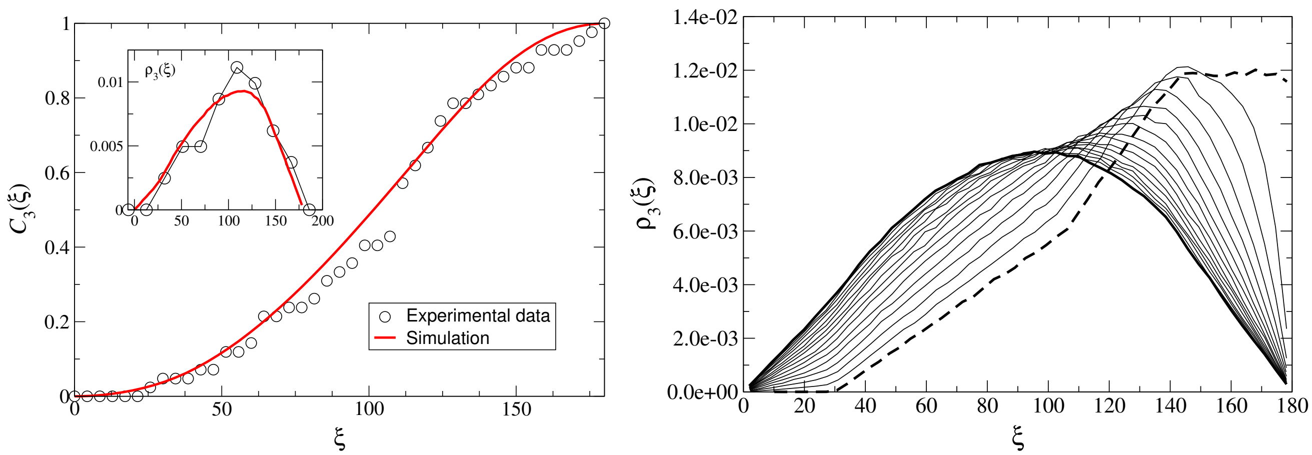

(a) (b)

Figure 1: *(a)* Experimental cumulative distribution of the ξ angles (circles) and normalized histogram (inset, circles). The red lines are the result of a simulation performed according to the distributions $\rho_1(\phi)$ and $\rho_2(\theta)$ calculated from the experimental data. *(b)* Normalized histograms of the ξ angles from simulations performed at different values of σ_θ, from $\sigma_\theta = 0.001$ (thick dashed line) to $\sigma_\theta = 150$ (thick solid line).

Let us consider the hypotheses that underlie the interpretation of our experimental data. It is useful to schematically re-list our assumptions in logical order: *(i)* legitimation to introduce a *reduced* distribution function by averaging on the coordinate $\psi = (\theta_1 + \theta_2)/2$, *(ii)* factorization in the space (ϕ_1, ϕ_2, θ), *(iii)* symmetry of the function $\rho_2(\theta)$ around $\theta = 180^\circ$, *(iv)* doubling of the Fab–Fc angles population, $\phi_1 = \phi_2 = \phi$. By construction, the distribution $\rho_3(\xi)$ is not directly used to deduce the effective potential. Therefore, it is in principle possible to recover the information contained in the statistics of the Fab–Fab angles in order to assess *a posteriori* the correctness of the hypotheses built in our model. We proceeded as follows.

We first generated a large number of triplets (ϕ_1, ϕ_2, θ) drawn from the best–fit distributions $\rho_1(\phi)$ and $\rho_2(\theta)$, each triplet corresponding to a certain (possible) orientation of the two Fab arms with respect to the Fc stem. At each point we calculated the corresponding value of ξ. Lastly, we calculated the corresponding histogram and cumulative distribution of the ξ values. The result of this test is plotted in Fig. 1 *a*, showing a very good agreement of the simulation with the experimental distribution. We conclude that there are no potential energy terms responsible for the observed distribution of the Fab–Fab angles. Rather, the latter may be regarded as originating from two different kinds of constraints imposed by the molecular structure. On one side, the excluded volume effects of the Fab–Fab and Fab–Fc interactions result in the appearance of the experimental cutoffs $\phi_{\min} \approx 15^\circ$ and $\phi_{\max} \approx 127.6^\circ$. On the other side, the distribution $\rho_2(\theta)$ must have a standard deviation in the neighborhood of the experimental σ_θ to produce the observed $\rho_3(\xi)$ in combination with the distribution $\rho_1(\phi)$, namely $\sigma_\theta \approx 90^\circ$. This fact is illustrated by the curves shown in Fig. 1 *b*, which are produced in obeyance to the same geometrical constraints, but at different values of σ_θ.

In conclusions, we can interpret the results of the above described test as a proof of coherence of our theoretical framework.